fire

MDPI

Communication

Kinetic Study of Pyrolysis of Coniferous Bark Wood and Modified Fir Bark Wood

Olga Yu. Fetisova [1], Nadezhda M. Mikova [1], Anna I. Chudina [1] and Aleksandr S. Kazachenko [1,2,3,*]

[1] Institute of Chemistry and Chemical Technology, Krasnoyarsk Scientific Center, Siberian Branch, Russian Academy of Sciences, Akademgorodok 50, Bld. 24, 660036 Krasnoyarsk, Russia
[2] School of Nonferrous Metals and Materials Science, Siberian Federal University, pr. Svobodny 79, 660041 Krasnoyarsk, Russia
[3] Department of Biological Chemistry with Courses in Medical, Pharmaceutical and Toxicological Chemistry, Krasnoyarsk State Medical University, St. Partizan Zheleznyak, Bld. 1, 660022 Krasnoyarsk, Russia
* Correspondence: leo_lion_leo@mail.ru

Abstract: We report on the kinetics of pyrolysis of bark wood of four coniferous tree species: fir (*Abies sibirica*), larch (*Larix sibirica*), spruce (*Picea obovata*), and cedar (*Pinus sibirica*) denoted as FB, LB, SB, and CB, respectively. Thermogravimetry (TG) and differential scanning calorimetry (DSC) methods were used to study the influence of KCl and K_3PO_4 compounds on the process of thermal decomposition of fir bark and determine the main thermal effects accompanying this process. As a result of the studies carried out, it was found that KCl additives practically do not affect the decomposition of hemicelluloses, but they shift the maximum decomposition of the cellulose peak in the direction of decreasing temperature to 340.9 °C compared to untreated bark (357.5 °C). K_3PO_4 promotes the simultaneous decomposition of hemicelluloses and cellulose in the temperature range with a maximum of 277.8 °C. In both cases, the additions of KCl and K_3PO_4 reduce the maximum rate of weight loss, which leads to a higher yield of carbon residues: the yield of char from the original fir bark is 28.2%, in the presence of K_3PO_4 and KCl it is 52.6 and 65.0%, respectively. Using the thermogravimetric analysis in the inert atmosphere, the reaction mechanism has been established within the Criado model. It is shown that the LB, SB, and CB thermal decomposition can be described by a two-dimensional diffusion reaction (D2) in a wide range (up to 0.5) of conversion values followed by the reactions with orders of three (R3). The thermal decomposition of the FB occurs somewhat differently. The diffusion mechanism (D2) of the FB thermal decomposition continues until a conversion value of 0.6. As the temperature increases, the degradation of the FB sample tends to R3. It has been found by the thermogravimetric analysis that the higher cellulose content prevents the degradation of wood. The bark wood pyrolysis activation energy has been calculated within the Coats–Redfern and Arrhenius models. The activation energies obtained within these models agree well and can be used to understand the complexity of biomass decomposition.

Keywords: coniferous bark wood; modified fir bark wood; pyrolysis; thermogravimetric analysis (TGA); differential scanning calorimetry (DSC); activation energy

Citation: Fetisova, O.Y.; Mikova, N.M.; Chudina, A.I.; Kazachenko, A.S. Kinetic Study of Pyrolysis of Coniferous Bark Wood and Modified Fir Bark Wood. *Fire* **2023**, *6*, 59. https://doi.org/10.3390/fire6020059

Academic Editors: Mingjun Xu, Ruiyu Chen and Man Pun Wan

Received: 14 December 2022
Revised: 20 January 2023
Accepted: 4 February 2023
Published: 8 February 2023

1. Introduction

Bark is the carbon-containing solid waste material most widespread in woodworking and pulp and paper industries. In Russia, 68–74 million m^3 of wood waste is generated annually, and according to the proceedings of the Biofuel congress held in St. Petersburg in 2019, the global growth of biomass in the form of waste amounts to 220 billion tons. At present, more than half of the bark waste is incinerated or stored, and the rest serves as an inexpensive energy source in pulp and paper mills or is composted for use in agriculture. At the same time, there is growing interest in using the bark of coniferous tree species as an essential component of biomass as a promising lignocellulosic source of organic carbon, which has significant potential for the sustainable production of porous carbon materials

and carbon adsorbents due to availability and relatively low cost. Bark can be used in agriculture to produce bark compost and in the tanning and extraction industry to extract tannins, which are used in the leather industry for tanning leather (turning raw leather into tanned). Due to the presence of valuable extractive substances in the bark, it can be used in medicine.

Pyrolysis is a promising technology for the conversion of biomass into fuel and chemicals [1–5]. Biomass pyrolysis can be defined simply as thermal decomposition of biomass without oxygen at moderate temperatures (400–600 °C). In addition, pyrolysis is the initial stage of biomass combustion, gasification, and liquefaction. Therefore, the knowledge of the pyrolysis parameters and kinetics is vital for predicting biomass behavior in the design and management of conversion plants.

Biomass mainly consists of cellulose, hemicelluloses, lignin, extractives, and small amounts of inorganic components, including alkali and alkaline earth metals. The interaction between alkaline and alkaline earth elements and organic components present in wood affects the pyrolysis mechanism by catalyzing or inhibiting chemical reactions leading to different amounts of coal, liquid, and gaseous products, as well as changing their composition [6]. It is known that the modern mechanism of pyrolysis has a number of disadvantages, namely, low efficiency and a high degree of contamination of the resulting products, which hinder their further use. The presence of substances catalyzing pyrolysis will help in solving these problems [7–9]. Particular attention of researchers is directed to potassium salts for their catalytic effect [10–14]. In [15], the authors found that the presence of potassium chloride changes the mechanism of cellulose pyrolysis. In particular, shifting the TG and DTG curves in the region of the main decomposition toward low temperatures, thereby showing the catalytic effect of potassium chloride. The study [16] presented data on the study of poplar pyrolysis with the addition of potassium salts. The results showed that potassium salts significantly accelerate the conversion time and significantly shift the exothermic peak. Chen [17] studied the microwave pyrolysis of sawdust of eight kinds of inorganic salts at 470 °C. It was found that inorganic salts greatly increase the yield of the solid product, reduce the yield of the gaseous product, and have no obvious effect on the yield of the liquid product. Hwang [18] studied the pyrolysis of poplar impregnated with potassium at a temperature of 450 °C, 500 °C, and 550 °C. Potassium has been found to increase the yield of char and affect the properties of the pyrolysis oil. In [19], the effect of K_2CO_3 on pine sawdust was studied, where a K_2CO_3 catalyst was added and the pyrolysis temperature was increased, the content of high-quality H_2 in the synthesis gas increased, and oxygenates in the pyrolysis oil decreased. As can be seen, there is enough information in the literature on the catalytic effect of potassium compound additives, and this information is sometimes contradictory. The results indicate that the process of activation of the lignocellulosic precursor by various potassium compounds is complex. A possible change in the composition of the activator during the heat treatment of the lignocellulosic precursor may change their mode of action. In addition, the thermal behavior of fir tree bark, which is often found in the forests of many countries, has not been systematically studied.

A study of the kinetic regularities of the investigated processes makes it possible to establish features of the pyrolysis mechanism and find an approach to choosing its parameters. The main kinetic parameters of biomass pyrolysis (the reaction order and activation energy) can be estimated by analyzing the thermogravimetry (TG) curves [20,21]. To do that, different kinetic calculation methods have been developed, including model-free (isoconversional) ones, which do not require a reaction model, and model-fitting ones, in which a reaction model should be chosen. In the model-free methods (Kissinger, Flynn–Wall–Ozawa, and Kissinger–Akahira–Sonuse), the kinetic parameters are calculated at the same conversion value using different kinetic curves at different heating rates. To determine correctly the kinetic parameters using such methods, experimental data should be processed using at least three thermoanalytical measurements performed at different heating rates, which, of course, makes the experiments too time-consuming.

The Arrhenius, Coats–Redfern, Horowitz–Metzger, Freeman–Carroll, etc. methods are model-fitting. In these methods, one thermoanalytic measurement is sufficient; however, several sets of kinetic parameters can correspond to different kinetic mechanisms describing the thermoanalytic curve. Generally, the problem of determining the constants is reduced to fitting a mathematical model of the reaction rate to the experimental kinetic curve or its individual portions.

The kinetic simulation of thermal decomposition is of great importance for the accurate prediction of the behavior of a material under different operation conditions [22]. Pyrolysis of wood is a complex chemical process that involves several simultaneous reactions. Understanding the effect of the process conditions and the initial biomass characteristics on the parameters of the thermal decomposition products can help in the design, operation, and optimization of the processes and equipment. The improvement of the description of the kinetic pyrolysis reactions can reduce the cost of the thermochemical conversion.

The aim of this study was to explore the pyrolysis kinetics of the bark of four coniferous trees growing in Siberia (Russia). In addition, the effect of compounds with the same potassium cation on the thermochemical transformation of fir bark under conditions of dynamic pyrolysis was studied. Based on the thermogravimetric analysis, the process was studied using the kinetic equations of the Coates–Redfern and Arrhenius methods. A possible pyrolysis mechanism was studied using the Criado method.

2. Materials and Methods

Samples of fir (*Abies sibirica*), larch (*Larix sibirica*), spruce (*Picea obovata*), and cedar (*Pinus sibirica*), denoted as FB, LB, SB, and CB, respectively, were used as raw materials. The samples were crushed and sieved with sieve mesh no. 70–170. Since the bark contains a great number of extractives [23], the samples were preliminarily subjected to the Soxhlet extraction with an ethanol-toluene mixture (1:2 vol./vol.) for 8 hours. The extractive contents were 19.5, 15.7, 18.3, and 16.9 wt % for the FB, LB, SB, and CB samples, respectively. After that, the samples were dried at 80°C for more than 6 h. The bark moisture content before drying was 4–6 wt %. The ash content was determined using the standard TAPPI T211 method based on calcination of the sample in air at 525 °C.

The content of lignin in the bark was determined by the gravimetric method [24]. For this purpose, the sample was hydrolyzed with sulfuric acid (72 wt. %) at 20 °C for 2.5 h. Then the reaction mixture was diluted with water (up to a concentration of sulfuric acid of 4 wt. %) and boiled for 1 h. Lignin was separated by filtration, washed to a neutral pH, and dried at 105 °C to a constant weight.

The content of cellulose in the bark samples was determined by the gravimetric method of Kurshner and Hanack [25] with modification [26]. Briefly, a sample (1.0 g) was gently refluxed (30 min) with 50 ml acetic acid:H_2O:HNO_3 at the volume ratios (8:2:1) in a flask equipped with a reflux condenser. After cooling, the insoluble residue was filtered through a paper filter (dried to constant weight) under vacuum, washed with distilled water until neutral pH, then with ethanol (96%). The resulting residue was dried in a laboratory oven at 50 °C to constant weight. The resulting pulp was corrected for ash content.

Analytically pure compounds KCl and K_3PO_4 (chemically pure) were used as K-containing agents; solutions of the required concentration were prepared using distilled water. Fir bark was modified with various potassium compounds by impregnating starting material (according to moisture capacity) with aqueous solutions of potassium compounds at the same mass ratio (1:0.5). The dried modified samples were named according to the activator used: FB/KCl, FB/K_3PO_4. As a reference sample, FB was used without any additional deposition of metal.

The pyrolysis of the initial and modified (with potassium compounds) biomasses was implemented with a NETZSCH STA 449 F1 Jupiter thermal analyzer. A sample of 15–16 mg was loaded into the analyzer and heated from 25 to 900 °C at a rate of 10 °C/min.

The high-purity carrier argon gas was supplied at a flow rate of 50 mL/min. The TGA experiments were repeated 3 times; the weight loss curves were found to be similar.

The general kinetic model describing the degradation during the nonisothermal pyrolysis is

$$\frac{d\alpha}{dt} = Ae^{-\frac{E}{RT}} \cdot f(\alpha) \quad (1)$$

where E is the apparent activation energy (kJ/mol), R is the gas constant (8.314 kJ/mol), A is the pre-exponential factor (min^{-1}), T is the absolute temperature (K), α is the conversion, t is the time (min), and $f(\alpha)$ is the function that represents the reaction model and depends on the reaction mechanism (see Table 1).

Table 1. Expressions of the $f(\alpha)$ and $g(\alpha)$ functions based on different reaction mechanisms.

Reaction Mechanism	$f(\alpha)$	$g(\alpha)$
Diffusion models		
D1 diffusion (1D)	$1/2\alpha$	α^2
D2 diffusion, Valensi (2D)	$[-\ln(1-\alpha)]^{-1}$	$\alpha + (1-\alpha)\ln(1-\alpha)$
D3 diffusion, Jander (3D)	$(3/2)\,(1-\alpha)^{2/3}/[1-(1-\alpha)^{1/3}]$	$[1-(1-\alpha)^{1/3}]^2$
D4 diffusion, Ginstling (3D)	$(3/2)/[(1-\alpha)^{-1/3}-1$	$1-2\alpha/3-(1-\alpha)^{2/3}$
Random nucleation and nuclei growth		
A1 Avrami–Erofeev	$3/2(1-\alpha)[-\ln(1-\alpha)]^{1/3}$	$[-\ln(1-\alpha)]^{2/3}$
Geometrical contraction models		
Phase boundary-controlled reaction (contracting area) (F2)	$2(1-\alpha)^{1/2}$	$1-(1-\alpha)^{1/2}$
Phase boundary-controlled reaction (contracting volume) (F3)	$3(1-\alpha)^{2/3}$	$1-(1-\alpha)^{1/3}$
Reaction order		
R1 First order	$1-\alpha$	$-\ln(1-\alpha)$
R2 Second order	$(1-\alpha)^2$	$(1-\alpha)^{-1}-1$
R3 Third order	$(1-\alpha)^3$	$[(1-\alpha)^{-2}-1]/2$
R1.5 One and half order	$(1-\alpha)^{3/2}$	$2[(1-\alpha)^{-1/2}-1]$

The activation energies of the biomass pyrolysis were obtained by the 2 model-fitting methods: Coats–Redfern and Arrhenius.

The conversion during the pyrolysis process can be written as

$$\alpha = \frac{m_i - m_a}{m_i - m_f} \quad (2)$$

Here, m_i, m_a, and m_f are the initial, actual, and final sample weights, respectively.

In the case of the nonisothermal thermogravimetry at a linear heating rate of $\beta = dT/dt$, Equation (1) can be transformed into the relation

$$\frac{d\alpha}{dT} = \frac{A}{\beta}e^{-\frac{E}{RT}} \cdot f(\alpha) \quad (3)$$

A solid-state reaction model was predicted by the Criado method [27–29]. In this method, the mechanism of the solid-state reaction occurring during the thermal degradation of woody biomass is determined from the theoretical curves obtained from the left-hand side of the equation:

$$\frac{Z(\alpha)}{Z(0.5)} = \frac{f(\alpha)\cdot g(\alpha)}{f\alpha(0.5)\cdot g(0.5)} = \left(\frac{T_\alpha}{T_{0.5}}\right)^2 \cdot \left(\frac{\left(\frac{d\alpha}{dt}\right)_\alpha}{\left(\frac{d\alpha}{dt}\right)_{0.5}}\right) \quad (4)$$

The theoretical curves are derivatives of the $g(\alpha)$ and $f(\alpha)$ functions, the algebraic expressions of which are given in Table 1. The experimental curve is obtained using the

right-hand side of Equation (4). By comparing experimental and theoretical curves, the type of mechanism involved in the thermal degradation can be identified.

2.1. Arrhenius Model

Using Equation (3), the apparent activation energy E could be obtained from the plot of $\ln[(d\alpha/dT)/f(\alpha)]$ versus $1/T$. The expressions for $f(\alpha)$ are listed in Table 1. The activation energy is calculated from the slope—E/R.

2.2. Coats–Redfern Model

The Coats–Redfern method is integral model-fitting. Solving Equation (3) using the asymptotic approximation ($2RT/E << 1$), we obtain the equation

$$ln\left(\frac{g(\alpha)}{T^2}\right) = ln\frac{AR}{\beta E}\left(1 - 2\frac{RT}{E}\right) - \frac{E}{RT} \quad (5)$$

where $g(\alpha)$ is the integral reaction model. The expressions for $g(\alpha)$ are listed in Table 1.

3. Results and Discussion

3.1. Thermogravimetry Analysis

Figure 1 shows the thermogravimetry (TG) (a) and differential thermogravimetry (DTG) (b) profiles of the FB, LB, SB, and CB pyrolysis at a heating rate of 10 °C/min.

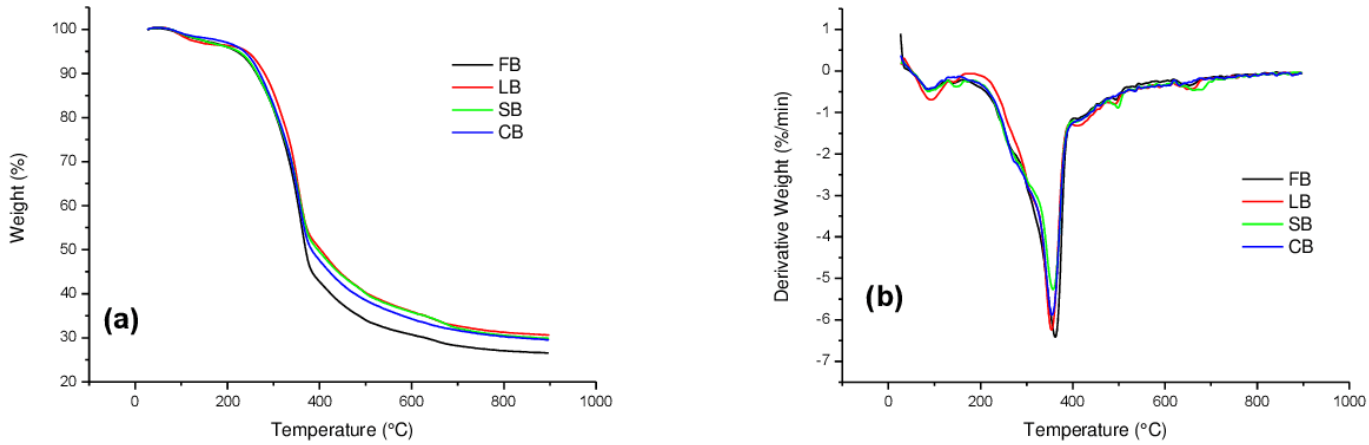

Figure 1. TGA analysis of pyrolysis of bark wood: TG (**a**) and DTG (**b**) curves.

The curves have the typical appearance of pyrolysis of lignocellulosic materials. The thermal decomposition of bark samples started at about 200 °C, followed by a major loss of weight in the temperature range of 200 and 380 °C, during which the bulk of the volatiles was released, and it was essentially completed by 700 °C, with the evolution of secondary gases, leading to the formation of char. The amount of char obtained for FB, LB, SB, and CB is 28.2, 32.6, 32.1, and 31.7%, respectively. By the end of pyrolysis (700 °C), the fir bark showed a greater weight loss compared to other studied bark samples, which indicates a higher content of the carbohydrate component.

In the faster step of the conversion process, two distinct peaks are clearly observed in all the DTG curves. The first, occurring at lower temperatures, represents the decomposition of hemicellulose present in each material, and the second corresponds to the decomposition of cellulose. For the flat tailing section, lignin is responsible, which is known to decompose slowly over a broader temperature range [30,31].

By comparing the DTG peaks (Figure 1b) between investigated bark woods, it can be noticed that they are similar in position but differ in height. The maximum decomposition rate decreases in a row: FB, LB, CB, and SB (6.5, 6.3, 5.9, and 5.3%/min, respectively). It can

be assumed that the rate of decomposition of the main period of pyrolysis of the bark of wood is associated with the content of cellulose, as noted in [32].

The biomass composition was determined chemically using the procedure described in detail in Section 2. The analytical data obtained are given in Table 2.

Table 2. Bark wood composition (wt %, dry and extractive-free basis) determined by the chemical method.

Sample	Chemical Composition (%)			Ash (%)
	Cellulose	Lignin	Hemicelluloses *	
FB	29.4	35.5	32.7	2.4
LB	29.3	38.8	29.3	2.5
CB	28.2	43.9	25.1	2.8
SB	22.0	42.3	31.8	3.8

* Calculated by the difference: 100%—cellulose, lignin, and ash content.

According to the data given in Table 2, FB has the highest cellulose content. The cellulose content decreases in the range: FB—LB—CB—SB, which corresponds with the range of the maximum rate of mass loss during the main decomposition.

The comparison of the chemical (Table 2) and DTG analysis data (Figure 1b) shows that the cellulose content is related to the biomass thermal stability and decomposition rate. The higher the cellulose content, the higher the rate and temperature of the thermal decomposition of the material.

3.2. Activation of Fir Bark by Potassium Compounds

Since the nature of the thermal decomposition of FB differs from other biomass samples studied in this work, the effect of modifying additives KCl and K_3PO_4 on the efficiency and selectivity of its pyrolysis was studied. Figure 2a shows the derivatives of thermogravimetric curves of mass loss (DTG curves), which allow determining the temperatures of the maximum rates of thermal decomposition of bark samples impregnated with KCl and K_3PO_4. The difference in decomposition temperatures of FB/KCl and FB/K_3PO_4 from the original bark (FB) at the initial stage of pyrolysis was noted. So, if for the FB a 3% decrease in mass associated with the predominant removal of moisture and thermally unstable low-molecular components occurs by 140 °C, then for the FB/KCl it is only at a temperature close to 200 °C. In the case of the FB/K_3PO_4, the temperature of the initial (3%) mass loss, on the contrary, occurs earlier—at 115 °C. Perhaps the earlier weight loss is associated with the removal of crystallization water, which is part of the crystallohydrates of the type $K_3PO_4 \cdot nH_2O$ formed during impregnation. It is also likely that intensive removal of adsorbed and bound water from the bark occurs due to the strong dehydrating effect of potassium orthophosphate. On the DSC curves (Figure 2b), endothermic peaks with maximum value at ~90–116 °C correspond to this stage of weight loss.

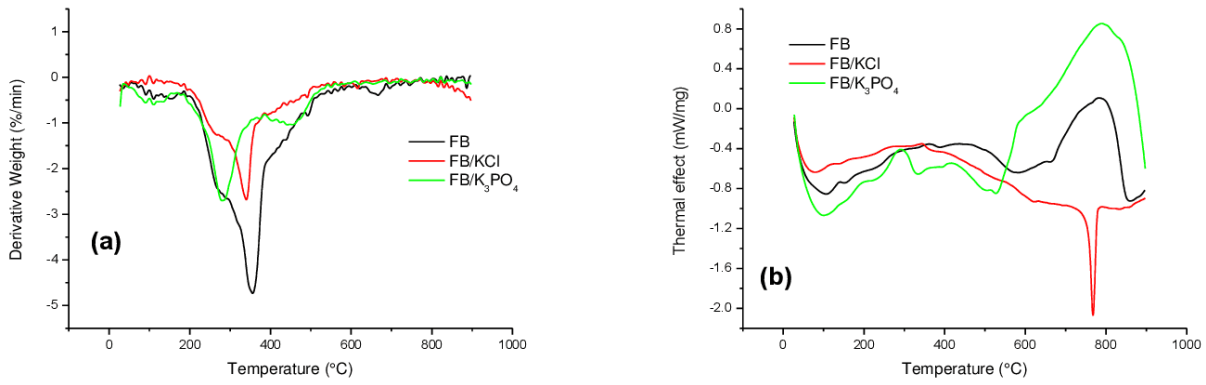

Figure 2. TGA/DSC analysis of pyrolysis of FB, FB/KCl, and FB/K_3PO_4: DTG (**a**) and DSC (**b**) curves.

The main thermal decomposition process for the studied samples becomes more intense after 200 °C, increases to ~360 °C, and is mostly completed by 520 °C. Table 3 presents the main characteristics of the thermal decomposition process of the studied samples: conditional intervals in which the predominant decomposition of the material is observed, maximum rate of mass loss (V_{max}), maximum mass loss temperatures (T_{max}), weight loss in this temperature range (Δm).

Table 3. The main parameters of thermal decomposition of FB, FB/KCl, and FB/K_3PO_4.

Sample	Interval, °C	V_{max}, %/min	T_{max}, °C	Δm
FB	140–280	1.01	~260	14.30
	280–400	3.93	357.5	38.60
	400–520	1.08	460.0	12.60
FB/KCl	200–280	1.25	263.0	6.90
	280–380	2.74	340.9	16.41
	380–500	0.58	-	7.00
FB/K_3PO_4	117–240	0.60	-	7.20
	240–360	2.72	277.8	23.05
	360–520	1.12	440.4	13.25

With the thermal decomposition of FB between 280 and 400 °C, the most significant reduction in mass (23.6%) occurs in the range of 320–380 °C at a rate of 3.93%/min and at a temperature of the maximum rate of mass loss of 357.5 °C. The FB/KCl shows a similar behavior during thermal degradation, which indicates a relatively uniform nature of the decomposition of components of lignocellulose biomass. Corresponding to the temperature range between 220 and 380 °C, a relatively narrow and symmetrical profile on the DTG curve of the FB/KCl detects a shift of the "cellulose" peak in the direction of a decrease in temperature to 340.9 °C [33]. At the same time, the position of the maximum on the hemicelluloses shoulder (263 °C) has practically not changed. The rate of mass loss of 2.74%/min corresponded to the main stage of decomposition. A decrease in the maximum rate of mass loss under the influence of KCl is accompanied by a decrease in mass loss compared to FB (16.41 vs. 38.6%) and, accordingly, an increase in charcoal yield.

On the DSC curves (Figure 2b), describing at this stage the exothermic nature of the release of volatile products, peaks are recorded at 360.8 °C for the FB and at 341 °C for FB/KCl. The DTG curves of FB/K_3PO_4 show the presence of two peaks: the main one, with a maximum mass loss at a temperature of 277.8 °C and a shoulder of about 341 °C, and a less intense one at 440.4 °C. The predominant decomposition of FB/K_3PO_4 with a mass loss of 23.05% occurs in the main temperature range of 240–360 °C with a maximum mass loss rate of 2.72%/min, close to the decomposition rate of FB/KCl. On the DSC curve, an exothermic maximum at 310 °C corresponds to this stage of decomposition due to the predominant decomposition of hemicelluloses and cellulose. The comparison of the effect of additives KCl and K_3PO_4 showed that both salts in the main temperature range lower the temperature at which the predominant decomposition of cellulose occurs, reducing the maximum rate of mass loss and thereby promoting the formation of char.

However, their different effects on the pyrolytic decomposition of the crust are that KCl has practically no effect on the pyrolysis of hemicelluloses, which were manifested by a wide shoulder on the DTG curve at 260 °C, as in the case of the FB. At the same time, KCl has an effect on the destruction of lignin, restraining the rate of its decomposition. This is indicated by a decrease in mass loss (7.0%) and a slowdown in the average rate of its loss (0.53%/min) with a further increase in temperature up to 520 °C. The process proceeds without pronounced thermal extremes.

The effect of the presence of the activator K_3PO_4 is expressed in a decrease in the decomposition temperature of polysaccharides as a whole [34]. At the same time, the peaks of hemicelluloses and cellulose on the DTG curve merge into one with a maximum at 277.8 °C and an implicitly distinguishable shoulder at about 340 °C. The addition of K_3PO_4 also affects the subsequent stage of decomposition of the substance in the

range of 360–520 °C, accelerating the decomposition of lignin. On the DTG curve, there is a wide peak of the mass loss rate of 1.12%/min at 440.4 °C, and on the DSC curve, there is a peak of the exoeffect at 420 °C, characteristic of lignin [33]. A similar effect of K_3PO_4 additives on the example of thermal decomposition of lignocellulose materials was noted in [35], where it was shown that K_3PO_4 promotes the decomposition of lignin with the formation of phenols.

For FB, decomposition proceeds at a mass loss rate of 1.08%/min and is accompanied by an exoeffect on the DSC curve at 434.3 °C, which can characterize the temperature maximum of lignin decomposition [33,35]. At 520 °C, most of the substance in the compared samples is subjected to thermal decomposition and transformation. Further, up to 700–800 °C, the process of weight loss for all samples slows down (to 0.12–0.3 %/min) due to the formation of thermally more stable thermolysis products and generally ends by 700 °C with the formation of carbon residues from FB/ K_3PO_4, FB/KCl, and FB about 52.6, 65.0 and 28.2%, respectively. Thus, KCl and K_3PO_4, by reducing the yield of volatile substances at the main stage of thermal decomposition, contribute to an increase in the yield of the solid product.

In the case of FB, a wide endothermic peak on the DSC curve at 600 °C can characterize the process of coke formation in the structure of the coal matrix (see Figure 2b). At 775 °C, the DSC of the FB/KCl in the endothermic region reveals a narrow, intense melting peak of KCl [36]. The high-intensity peak on the DSC curve of FB/K_3PO_4 with a maximum of 780 °C probably characterizes the transformation and decomposition of a mixture of ortho- and polyphosphoric compounds.

Thus, under the influence of the treatment of fir bark with potassium chloride, both a decrease (compression) of the main range of decomposition of raw materials occurs and a shift in the temperature maximum of decomposition toward lower temperatures by 16.6 °C compared to the FB. At the same time, in the considered temperature range, K_3PO_4 had a greater effect on the shift temperature of the exothermic peak than KCl (277.8 versus 340.9 °C). Consequently, the results obtained in the study show that KCl and K_3PO_4 can significantly affect the process of thermal decomposition of fir bark, accelerating or suppressing individual stages of pyrolysis.

3.3. Results of the Kinetic Analysis

The mechanism of pyrolysis of bark wood was predicted from Criado's master plot. The Criado's curves were generated from Equation (4) by plotting $Z(\alpha)/Z(0,5)$ vs. conversion α (Figure 3a–d). The experimental data in Figure 3 shows that for all bark wood species studied in the range of α = 0.2–0.5, they directed between the D1, D2, D3, and D4 curves. By increasing the degree of conversion to 0.6, the experimental curves of FB, SB, and CB samples are still in the diffusion region. The fir bark sample is predominantly between D1 and D2, and the spruce and cedar bark samples overlap curves D2 and D4. According to the literature, these degradation mechanisms refer to a diffusion process in one, two, three, and four dimensions, respectively [37]. Similar results were described by [38–40] for other cellulosic fibers and [41] for hardwood and softwood. Based on this result, at lower conversion values, the heating transfer occurs by diffusion throughout the sample.

The experimental curve of the larch bark sample after the degree of conversion of 0.5 tends to the region of the reaction order mechanism (R2 and R3). For FB, CB, and SB, when the conversion value increases above 0.6, the shape of the experimental curve tends to follow the R3 mechanism, as shown in Figure 3. Thus, the reaction can be classified as a reaction order mechanism (2nd to 3rd): the reaction rate is proportional to the concentration, amount, or proportion of the remaining reactants raised in a certain reaction order [42]. Then bark wood reaction model can be considered as a diffusion type followed by a reaction order mechanism (R2 and R3).

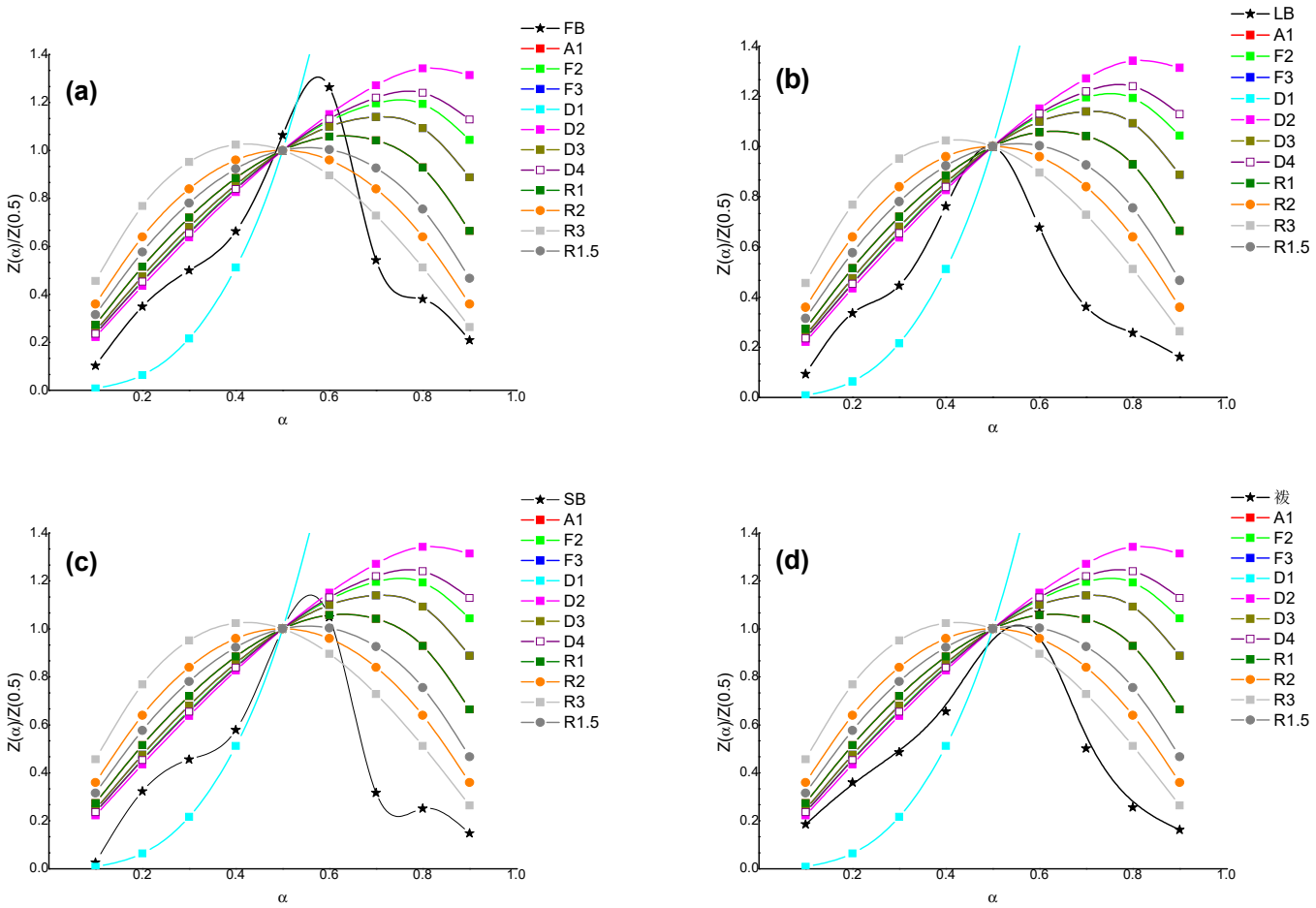

Figure 3. Theoretical and experimental plots for predicting the pyrolysis reaction mechanism by the Criado method (Z-master plot): (**a**) FB in the range of 246–501 °C, (**b**) LB in the range of 263–558 °C, (**c**) SB in the range of 247–567 °C, and (**d**) CB in the range of 252–537 °C.

Using the Criado method, a possible mechanism for the thermal decomposition of fir bark modified with KCl and K_3PO_4 was evaluated. From the experimental data in Figure 4a, it can be seen that the decomposition mechanism of the FB/KCl is almost the same as the FB. The difference is that the diffusion region passes into the order reaction model already after the degree of conversion of 0.5. With that, at a degree of conversion of 0.4–0.5, the mechanism coincides with the D1 diffusion model. At conversion values greater than 0.5, the mechanism predicted is a reaction of order R3. In other words, the reaction model pyrolysis of FB/KCl can be regarded as diffusion type followed by the reaction order mechanism.

The mechanism of thermal decomposition of FB/K_3PO_4 differs from the original FB (Figure 4b). The experimental curve up to a degree of conversion of 0.2 is in the diffusion region (D1, D2, D3, and D4). With an increase in the degree of conversion (0.3–0.7), the mechanism of thermal degradation passes into the region of ordinal reaction models (R1, R2, R3, and R1.5). At conversion values greater than 0.7, the curve is closer to the R1.5 degradation mechanism, which refers to the reaction order model with the order of reaction as 1.5.

The biomass decomposition mechanism was estimated by the Arrhenius and Coats–Redfern methods. These methods are also used to establish a reaction mechanism. Since many reactions take place in the process of pyrolysis, only the apparent values of the activation energy can be experimentally determined. Table 4 gives the activation energies and the most suitable degradation mechanisms listed in Table 1.

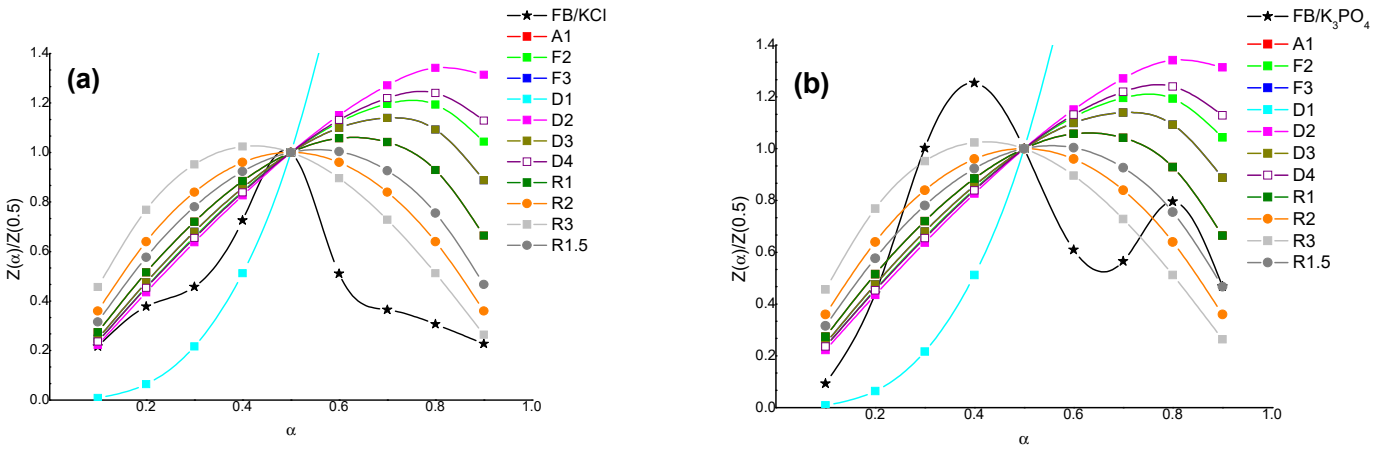

Figure 4. Theoretical and experimental plots for predicting the pyrolysis reaction mechanism by the Criado method (Z-master plot): (**a**) FB/KCl in the range of 237–617 °C, (**b**) FB/K_3PO_4 in the range of 152–497 °C.

Table 4. Activation energies of pyrolysis of the initial bark wood and fir bark wood modified by KCl and K_3PO_4 obtained by the Coats–Redfern and Arrhenius methods ($R^2 > 0.9$).

Sample	Temperature Range, °C	Coates–Redfern		Arrhenius	
		Mechanism	E_a	Mechanism	E_a
FB	261–346	D2	101	D2	99
	346–456	R3	87	R1.5	81
LB	277–352	D2	114	D2	110
	352–487	R3	90	R3	88
SB	262–347	D2	112	D1	115
	347–482	R3	73	R3	69
CB	262–347	D2	101	D1	97
	347–477	R3	76	R3	70
FB/KCl	237–337	D3	82	D2	80
	337–617	R3	43	R3	47
FB/K_3PO_4	152–237	D2	23	D2	20
	267–392	R3	44	R3	45
	442–497	R1.5	34	R1.5	38

For all studied samples of the original wood bark, the values of activation energy in diffusion and reaction order models are different. This is due to different mechanisms of thermal decomposition in the indicated intervals. The maximum activation energy in the diffusion (114 kJ/mol) and reaction order (90 kJ/mol) region is exhibited by LB, which indicates a high thermal stability of this sample. FB and CB in the diffusion region have the lowest activation energy (101 kJ/mol). The different thermal stability of the carbohydrate part of the woody substance of coniferous species is apparently due to the content and chemical composition of hemicelluloses, their interaction with cellulose and lignin, and the degree of cellulose crystallinity. In addition, light porous fir wood (density 350 kg/m^3) is better exposed to thermal decomposition (combustion) than, for example, denser larch wood (635 kg/m^3) [43].

After treatment with potassium salts, the activation energy of fir bark pyrolysis significantly decreases, which indicates a change in the biomass structure. Under the action of KCl, both the temperature interval of the diffusion mechanism and the activation energy decrease (from 114 for the FB to 82 for the FB/KCl). At the same time, in the conversion degree range of 0.5–0.9, the structure of the FB/KCl undergoes more significant changes since the activation energy is two times lower than that of the initial bark (from 87 to 43 kJ/mol) [44].

The introduction of K_3PO_4 has a more significant effect on the structure of the fir bark compared with KCl. First, the introduction of K_3PO_4 into the biomass structure significantly reduces the activation energy during pyrolysis due to the formation of a larger number of thermally less stable structural regions. Secondly, already after the degree of conversion 0.2, the mechanism of degradation of the fir bark changes from a diffusion character to an order reaction. Moreover, up to a degree of conversion of 0.7, the mechanism of thermal decomposition is similar to the initial bark (R3). In the temperature range 442–497 °C, where lignin is predominantly decomposed, the decomposition mechanism is described by the reaction order model with the order of reaction as 1.5 (R1.5).

4. Conclusions

Pyrolysis of the coniferous bark wood was characterized using the thermogravimetry analysis. The interrelation between the biomass components and the mechanism of their thermal decomposition was established. It was found that decomposition in the temperature range corresponding to cellulose destruction is diffusion-assisted. It was noted that the rate of decomposition of the main period of wood bark pyrolysis is related to the content of cellulose. The pyrolysis of bark wood proceeds via diffusion with conversion values below 0.5 for the SB, LB, and CB samples. The diffusion-assisted decomposition of the FB sample continues until a conversion value of 0.6, which is probably due to the high cellulose content. Upon further heating, the thermal decomposition of bark wood tends to model third-order reactions. Using the Coates–Redfern and Arrhenius methods, the activation energies of the main sample thermal decomposition stages were determined. The relationship between the intensity of weight loss of the substance and the degree of thermal decomposition of the original and modified with KCl and K_3PO_4 fir bark was studied by the TG/DTA method. DSC analysis determined the main thermal effects accompanying the pyrolysis process. It was found that under the action of the treatment of the bark with KCl, a shift in the temperature maximum of decomposition by 16.6 °C toward lower temperatures (340.9 °C) is observed in comparison with the untreated bark (357.5 °C). It has been suggested that KCl has practically no effect on the pyrolysis of hemicelluloses, but it inhibits the decomposition of lignin. The presence of K_3PO_4 promotes earlier degradation of polysaccharides; the peaks of cellulose and hemicelluloses on the DTG curve practically merge into one with a maximum at 277.8 °C. The decomposition of lignin under the influence of K_3PO_4 occurs more intensively. It has been shown that additions of KCl and K_3PO_4 lower the temperature of predominant decomposition of cellulose, reduce the maximum rate of weight loss, and thereby contribute to a greater yield of carbon residues: in the case of samples from FB/K_3PO_4, about 52.6%, FB/KCl, 65.0%, and from the original bark (FB)—28.2%.

Author Contributions: Formal analysis, writing–original draft preparation, O.Y.F.; investigation, N.M.M.; investigation, A.I.C.; investigation, resources, A.S.K. All authors have read and agreed to the published version of the manuscript.

Funding: This study was carried out within the budget plan # 0287-2021-0017 for the Institute of Chemistry and Chemical Technology, Siberian Branch of the Russian Academy of Sciences.

Data Availability Statement: All data generated during this study are included in the article.

Acknowledgments: This study was carried out using the equipment of the Krasnoyarsk Regional Center for Collective Use of the Krasnoyarsk Scientific Center, Siberian Branch of the Russian Academy of Sciences.

Conflicts of Interest: The authors declare no conflict of interest.

References

1. Ding, Y.; Huang, B.; Li, K.; Du, W.; Lu, K.; Zhang, Y. Thermal interaction analysis of isolated hemicellulose and cellulose by kinetic parameters during biomass pyrolysis. *Energy* **2020**, *195*, 117010. [CrossRef]
2. Lin, B.; Zhou, J.; Qin, Q.; Song, X.; Luo, Z. Thermal behavior and gas evolution characteristics during co-pyrolysis of lignocellulosic biomass and coal. *J. Anal. Appl. Pyrolysis* **2019**, *144*, 104718. [CrossRef]
3. Fermanelli, C.S.; Córdoba, A.; Pierella, L.B.; Saux, C. Pyrolysis and copyrolysis of three lignocellulosic biomass residues from the agro-food industry: A comparative study. *Waste Manag.* **2019**, *102*, 362–370. [CrossRef] [PubMed]
4. Chen, X.; Che, Q.; Li, S.; Liu, Z.; Yang, H.; Chen, Y.; Wang, X.; Shao, J.; Chen, H. Recent developments in lignocellulosic biomass catalytic fast pyrolysis: Strategies for the optimization of bio-oil quality and yield. *Fuel Process. Technol.* **2019**, *196*, 106180. [CrossRef]
5. Mian, I.; Li, X.; Jian, Y.; Dacres, O.D.; Zhong, M.; Liu, J.; Ma, F.; Rahman, N. Kinetic study of biomass pellet pyrolysis by using distributed activation energy model and Coats Redfern methods and their comparison. *Bioresour. Technol.* **2019**, *294*, 122099. [CrossRef]
6. Perander, M.; DeMartini, N.; Brink, A.; Kramb, J.; Karlström, O.; Hemming, J.; Moilanen, A.; Konttinen, J.; Hupa, M. Catalytic effect of Ca and K on CO2 gasification of spruce wood char. *Fuel* **2015**, *150*, 464–472. [CrossRef]
7. Shah, M.; Dai, J.J.; Guo, Q.X.; Fu, Y. Products and production routes for the catalytic conversion of seed oil into fuel and chemicals: A comprehensive review. *Sci. China Chem.* **2015**, *58*, 1110–1121. [CrossRef]
8. Shen, Y.; Yoshikawa, K. Recent progresses in catalytic tar elimination during biomass gasification or pyrolysis-A review. *Renew. Sustain. Energy Rev.* **2013**, *21*, 371–392. [CrossRef]
9. Dickerson, T.; Soria, J. Catalytic fast pyrolysis: A review. *Energies* **2013**, *6*, 514–538. [CrossRef]
10. Liu, Y.; Wang, Y.; Guo, F.; Li, X. Characterization of the gas releasing behaviors of catalytic pyrolysis of rice husk using potassium over a micro-fluidized bed reactor. *Energy Convers. Manag.* **2017**, *136*, 395–403. [CrossRef]
11. Velasco, U.I.; Sierra, I.; Zudaire, L.; Ayastuy, J.L. Conversion of waste animal bones into porous hydroxyapatite by alkaline treatment: Effect of the impregnation ratio and investigation of the activation mechanism. *J. Mater. Sci.* **2015**, *50*, 7568–7582. [CrossRef]
12. Ouédraogo, I.W.K.; Mouras, S.; Changotade, O.A.; Blin, J. Development of a new solid catalyst for biodiesel production using local vegetable resources, adapted to the contexts of the west african countries. *Waste Biomass Valori.* **2018**, *9*, 1893–1901. Available online: https://link.springer.com/article/10.1007/s12649-017-9964-3 (accessed on 1 February 2023).
13. Ryczkowski, R.; Niewiadomski, M.; Michalkiewicz, B.; Skiba, E.; Ruppert, A.M. Effect of alkali and alkaline earth metals addition on Ni/ZrO2 catalyst activity in cellulose conversion. *J. Therm. Anal. Calorim.* **2016**, *126*, 103–110. [CrossRef]
14. Zhang, Y.; Gong, X.; Zhang, B. Potassium catalytic hydrogen production in sorption enhanced gasification of biomass with steam. *Int. J. Hydrog. Energy* **2014**, *39*, 4234–4243. [CrossRef]
15. Ferreiro, A.I.; Rabaçal, M.; Costa, M.; Giudicianni, P.; Grottola, C.M.; Ragucci, R. Modeling the impact of the presence of KCl on the slow pyrolysis of cellulose. *Fuel* **2018**, *215*, 57–65. [CrossRef]
16. Shah, M.H.; Deng, L.; Bennadji, H.; Fisher, E.M. Pyrolysis of potassium-doped wood at the centimeter and submillimeter scales. *Energy Fuels* **2015**, *29*, 7350–7357. [CrossRef]
17. Chen, M.-Q.; Wang, J.; Zhang, M.-X.; Chen, M.-G. Catalytic effects of eight inorganic additives on pyrolysis of pine wood sawdust by microwave heating. *J. Anal. Appl. Pyrol.* **2008**, *82*, 145–150. [CrossRef]
18. Hwang, H.; Oh, S.; Cho, I.G.; Choi, J.W. Fast pyrolysis of potassium impregnated poplar wood and characterization of its influence on the formation as well as properties of pyrolysis products. *Bioresour. Technol.* **2013**, *150*, 359–366. [CrossRef]
19. Zhou, W.; Bai, B.; Chen, G.; Ma, L.; Jing, D.; Yan, B. Study on catalytic properties of potassium carbonate during the process of sawdust pyrolysis. *Int. J. Hydrog. Energy* **2018**, *43*, 13829–13841. [CrossRef]
20. Barneto, A.G.; Vila, C.; Ariza, J.; Vidal, T. Thermogravimetric measurement of amorphous cellulose content in flax fibre and flax pulp. *Cellulose* **2011**, *18*, 17–31. [CrossRef]
21. Fetisova, O.Y.; Mikova, N.M.; Taran, O.P. Evaluation of the validity of model-fitting and model-free methods for kinetic analysis of nonisothermal pyrolysis of Siberian fir bark. *Kinet. Catal.* **2020**, *61*, 846–853. [CrossRef]
22. Doyle, C.D. *Techniques and Methods of "Polymer Evaluation"*; Marsel-Dekker: New York, NY, USA, 1966; Chapter 4.
23. Pásztory, Z.; Mohácsiné, I.R.; Gorbacheva, G.; Börcsök, Z. The utilization of tree bark. *BioResources* **2016**, *11*, 7859–7888.
24. Sluiter, A.; Hames, B.; Ruiz, R.; Scarlata, C.; Sluiter, J.; Templeton, D.; Crocker, D. *Determination of Structural Carbohydrates and Lignin in Biomass: Laboratory Analytical Procedure (LAP)*; National Renewable Energy Laboratory: Golden, CO, USA, 2008.
25. Kürschner, K.; Hanak, A. Zur Bestimmung der sog. Rohfaser. Ein neues Verfahren der Bestimmung der Rohcellulose in Kakao. *Z. Für Unters. Der Lebensmittel.* **1930**, *59*, 484–494. [CrossRef]
26. Ognyanov, M.; Remoroza, C.A.; Schols, H.A.; Petkova, N.T.; Georgiev, Y.N. Structural study of a pectic polysaccharide fraction isolated from "mountain tea" (*Sideritis scardica* Griseb.). *Carbohydr. Polym.* **2021**, *260*, 117798. [CrossRef] [PubMed]
27. Singh, S.; Prasad Chakraborty, J.; Kumar Mondal, M. Intrinsic kinetics, thermodynamic parameters and reaction mechanism of non-isothermal degradation of torrefied Acacia nilotica using isoconversional methods. *Fuel* **2020**, *259*, 116263. [CrossRef]
28. Mallick, D.; Poddar, M.K.; Mahanta, P.; Moholkar, V.S. Discernment of synergism in pyrolysis of biomass blends using thermogravimetric analysis. *Bioresour. Technol.* **2018**, *261*, 294–305. [CrossRef]
29. Criado, J.M. Kinetic analysis of DTG data from master curves. *Thermochim. Acta* **1978**, *24*, 186–189. [CrossRef]
30. Nhuchhen, D.R.; Basu, P. Experimental investigation of mildly pressurized torrefaction in air and nitrogen. *Energy Fuels* **2014**, *28*, 3110–3121. [CrossRef]

31. Maiti, S.; Purakayastha, S.; Ghosh, B. Thermal characterization of mustard straw and stalk in nitrogen at different heating rates. *Fuel* **2007**, *86*, 1513–1518. [CrossRef]
32. Damartzis, T.; Vamvuka, D.; Sfakiotakis, S.; Zabaniotou, A. Thermal degradation studies and kinetic modeling of cardoon (*Cynara cardunculus*) pyrolysis using thermogravimetric analysis (TGA). *Bioresour. Technol.* **2011**, *102*, 6230–6238. [CrossRef]
33. Patwardhan, P.R.; Satrio, J.A.; Brown, R.C.; Shanks, B.H. Influence of inorganic salts on the primary pyrolysis products of cellulose. *Bioresour. Technol.* **2010**, *101*, 4646–4655. [CrossRef] [PubMed]
34. Peng, C.-V.; Lin, H.C. Japanese cedar (*Cryptomeria japonica*) ash as a natural activating agent for preparing activated carbon. *J. Wood Sci.* **2015**, *61*, 316–325. [CrossRef]
35. Lu, Q.; Zhang, Z.B.; Yang, X.C.; Dong, C.Q.; Zhu, X.F. Catalytic fast pyrolysis of biomass impregnated with K_3PO_4 to produce phenolic compounds: Analytical Py-GC/MS study. *J. Anal. Appl. Pyrolysis* **2013**, *104*, 139–145. [CrossRef]
36. Chen, C.; Luo, Z.; Yu, C.; Wang, T.; Zhang, H. Transformation behavior of potassium during pyrolysis of biomass. *RSC Adv.* **2017**, *7*, 31319–31326. [CrossRef]
37. Criado, J.M.; Málek, J.; Ortega, A. Applicability of the master plots in kinetic analysis of non-isothermal data. *Thermochim. Acta* **1989**, *147*, 377–385. [CrossRef]
38. Wu, Y.; Dollimore, D. Kinetic studies of thermal degradation of natural cellulosic materials. *Thermochim. Acta* **1998**, *324*, 49–57. [CrossRef]
39. Bianchi, O.; Dal Castel, C.; Olivera, R.V.B.; Bertuoli, P.T.; Hillig, E. Nonisothermal degradation of wood using thermogravimetric measurements. *Polímeros* **2010**, *20*, 395–400. [CrossRef]
40. Poletto, M.; Pistor, V.; Zeni, M.; Zattera, A.J. Crystalline properties and decomposition kinetics of cellulose fibers in wood pulp obtained by two pulping processes. *Polym. Degrad. Stab.* **2011**, *96*, 679–685. [CrossRef]
41. Ding, Y.; Ezekoye, O.A.; Lu, S.; Wang, C.; Zhou, R. Comparative pyrolysis behaviors and reaction mechanisms of hardwood and softwood. *Energy Convers. Manag.* **2017**, *132*, 102–109. [CrossRef]
42. Khawam, A.; Flanagan, D.R. Solid-state kinetic models: Basics and mathematical fundamentals. *J. Phys. Chem. B* **2006**, *110*, 17315–17328. [CrossRef]
43. Borovikov, A.M.; Ugolev, B.N. *Handbook of Wood*; Forest Industry: Moscow, Russia, 1989; 244p.
44. Mikova, N.M.; Fetisova, O.Y.; Ivanov, I.P.; Chesnokov, N.V. Study of the thermochemical transformation of fir bark under conditions of its activation by potassium compounds. *Bull. Tomsk State Univ. Chemistry.* **2021**, *23*, 18–29. [CrossRef]